Palaeogeography, Palaeoclimatology, Palaeoecology 517 (2019) 74–85

Contents lists available at ScienceDirect

Palaeogeography, Palaeoclimatology, Palaeoecology

journal homepage: www.elsevier.com/locate/palaeo

Mid- to late-Holocene paleoenvironmental changes and glacier fluctuations reconstructed from the sediments of proglacial lake Buruo Co, northern Tibetan Plateau

Teng Xu[a,c,*], Liping Zhu[a,b,c,*], Xinmiao Lü[a,b], Qingfeng Ma[a], Junbo Wang[a,b], Jianting Ju[a], Lei Huang[a,c]

[a] Key Laboratory of Tibetan Environment Changes and Land Surface Processes (TEL), Institute of Tibetan Plateau Research (ITP), Chinese Academy of Sciences, Beijing 100101, China
[b] CAS Center for Excellence in Tibetan Plateau Earth Sciences, Beijing 100101, China
[c] University of Chinese Academy of Sciences, Beijing 100049, China

ARTICLE INFO

Keywords:
Lake Sediment
Grain-size
Palaeoclimate record
Westerlies
Solar insolation
Mid-Holocene

ABSTRACT

Glaciers on the Tibetan Plateau are an important freshwater resource for large populations in south and southeast Asia. Therefore, it is important to understand past variations in glacier activity in the region to assess their possible response to ongoing climatic warming. Here, we present the results of analyses of grain size, total organic carbon, pollen ratio (*Artemisia* to Chenopodiaceae) and the element content of a 435 cm-long sediment core from proglacial lake Buruo Co on the northern Tibetan Plateau. Our results indicate that the Buruo Co catchment experienced relatively warm and humid conditions during 5.2–4.0 cal kyr BP, during which retreating glaciers released large amounts of freshwater. Precipitation was also abundant during this interval as a result of the relatively strong Indian Summer Monsoon and weaker Westerlies and thus the lake level was high. During 4.0–1.3 cal kyr BP, the Westerlies were gradually enhanced and the climate became colder and drier; in response, the glaciers advanced and the lake level decreased. During 1.3–0 cal kyr BP, under relatively cold conditions, a large volume of glacial ice was maintained; nevertheless, under the Westerlies influence, the lake level rose. Four episodes of glacial advance are detected: at 3.6–3.4, 3.2–2.3, 1.9–1.7 and 0.4–0.1 cal kyr BP. These episodes correspond well with Bond events in the North Atlantic, implying that climate change and glacial activity at Buruo Co were largely driven by variations in Northern Hemisphere insolation and by climatic oscillations in the North Atlantic region, via the influence of the Westerlies.

1. Introduction

The Tibetan Plateau, which has been called “Earth's Third Pole” (Qiu, 2008) and the “Asian Water Tower” (Immerzeel et al., 2010), is highly sensitive to climatic change (An et al., 2001; Owen, 2009; Thompson et al., 2000). The Tibetan Plateau provides significant freshwater resources for most of the Asian population (Hou et al., 2017; Immerzeel et al., 2010); however, in recent decades the continuous melting of glaciers, under the influence of global warming (Oerlemans, 2005; Yao et al., 2012), has threatened the water security of the downstream region (Pritchard, 2017). Thus, it is essential to try to assess the future response of glaciers on the Tibetan Plateau to ongoing and future climate change. However, glacier activity is affected by numerous factors, such as solar irradiance (Joerin et al., 2006), winter precipitation (Vincent et al., 2005) and summer temperature (Loso, 2009); moreover, the processes by which glaciers respond to climate change in different climatic contexts are complex (Yao et al., 2012). Therefore, it is important to improve our understanding of the history of glacial activity under different environmental conditions, especially in the context of a probable warmer future.

The history of glacier activity has been widely reconstructed using moraine sequences (Liu et al., 2017) and proxies from ice cores (Thompson et al., 1997). The scale and intensity of glaciation can be determined by the spatial correlation of moraine chronology matters (Owen, 2009; Yi et al., 2008), but such reconstructions are always discontinuous and have relatively low temporal resolution. Proxies from ice cores can provide records of glacial activity with a high temporal resolution, but their duration and continuity may be limited given

* Corresponding authors at: Key Laboratory of Tibetan Environment Changes and Land Surface Processes (TEL), Institute of Tibetan Plateau Research (ITP), Chinese Academy of Sciences, Beijing 100101, China.
E-mail addresses: xuteng@itpcas.ac.cn (T. Xu), lpzhu@itpcas.ac.cn (L. Zhu).

https://doi.org/10.1016/j.palaeo.2018.12.023
Received 31 August 2018; Received in revised form 16 December 2018; Accepted 31 December 2018
Available online 03 January 2019
0031-0182/ © 2019 Elsevier B.V. All rights reserved.

that some glaciers may have completely melted during certain intervals in the past, even though they exist at the present.

Sedimentary records from proglacial lakes can provide valuable information on glacier activity during the Holocene (Karlén, 1976; Leonard, 1986). Lake sediment records are often continuous and Holocene glacial records have been widely recovered from proglacial lake sediment sequences, e.g. in Europe (Holzhauser et al., 2005; Joerin et al., 2006; Simonneau et al., 2014), Alaska (Loso et al., 2006) and in the Andes (Stansell et al., 2013). Such studies have also been conducted on the Tibetan Plateau, including in Muztagh Ata (Liu et al., 2014), Nianbaoyuze (Zhang and Mischke, 2009) and on the southeastern Tibetan Plateau (Huang et al., 2016). Liu et al. (2014) reconstructed a 4200-year record of glacier fluctuations in Muztagh Ata using the sediments of proglacial Kalakuli Lake, which is climatically influenced by the Westerlies. In the Nianbaoyuze Mountains, which are influenced by the Indian Summer Monsoon (ISM), glacial activity since the Last Glacial Maximum was reconstructed using grain size and geochemical proxies from the sediments of Ximencuo Lake (Zhang and Mischke, 2009). On the southeastern margin of the Tibetan Plateau, which is climatically controlled by the ISM, glacial fluctuations over the past ~8000 years in the catchment of Laigu Lake were reconstructed from sedimentary records of strontium (Sr), grain size and magnetic susceptibility (Huang et al., 2016).

Furthermore, current records show that glacier activity did not occur uniformly across the TP during the mid-late Holocene. Glacier activity is influenced by hydrothermal conditions combination which is different between the ISM and Westerlies. The various moisture sources of the main circulation systems may lead to a complex glacier response to climate change. Thus, it is essential to determine the spatial pattern of glacier activity on the Tibetan Plateau, in response to ongoing climate change. However, little is known about past glacier variations on the northern Tibetan Plateau, where the climate is influenced by the interaction of the ISM and the Westerlies, and the lack of continuous and high-resolution records from the region limits our understanding of its glaciation history and of the factors influencing climate change.

Here, we present the results of a high-resolution study of multiple environmental proxies from the sediments of Buruo Co, a proglacial lake located on the northern Tibetan Plateau, in the transition zone of the ISM and the Westerlies. The record spans the mid- to late-Holocene and we use it to reconstruct the history of glacier activity and climate change in the catchment during this interval.

2. Study area

Buruo Co (34°20′-34°28′N, 85°42′-85°49′E, 5170 m asl) is situated between the western slopes of the Zangsegangri Mountain and the eastern slopes of the Buruogangri Mountain in the central part of the Qiangtang Plateau, on the northern Tibetan Plateau (Fig. 1A, B). The study area has been called the “cold and dry core” of the Tibetan Plateau (Zheng, 1996) and is characterized by extremely cold, dry, windy and changeable weather with large temperature difference.

Buruo Co is a closed lake with a current surface area of 87.5 km^2 and catchment area of 550.5 km^2 (Wang and Dou, 1998). The maximum water depth exceeds 100 m according to a bathymetric survey carried out during field work in 2013 (Fig. 1C). Buruo Co is a type of mountain lake. There are many glacier tongues near the lake shoreline, extending from the western slopes of the Zangsegangri Mountain, and the resulting braided streams drain into the lake and strongly influence geomorphological processes along the lakeshore. The lake is fed mainly by water from melting snow and glacier ice (Wang and Dou, 1998), and has a replenishment coefficient of 6.3. Baihui River, the only perennial river in the catchment, is also mainly supplied by glacial meltwater from the northeastern part of the Buruogangri Mountain.

Buruo Co lies within the Qiangtang semi-arid climate zone. Observation data since 1973, from the nearest meteorological station in Gerze County, indicates that the mean annual temperature is 0.31 °C and the mean annual precipitation is 177.33 mm, with 93.8% of the total annual precipitation occurring from June to September (You, 2016). The prevalent modern vegetation type is alpine desert-steppe, typically consisting of *Carex moorcroftii*, *Ceratoides compacta*, *Saussurea* spp. and *Rhodiola* (Qinghai-Tibet Plateau Comprehensive Scientific Expedition Team of the Chinese Academy of Sciences, 1992).

The value of excess deuterium can provide information about the sources of moisture. In the Zangsegangri ice-core, the average value of excess deuterium was 16.82‰ (You, 2016), which is similar to that of the precipitation in central Asia controlled by the Westerlies but is substantially higher than that of the summer precipitation at Lhasa, which is controlled by the ISM (Tian et al., 2007). From these precipitation characteristics, we infer that the climate of the Buruo Co area is currently dominated by the Westerlies.

3. Materials and methods

3.1. Sediment cores

During October 2013 we conducted the first field investigation of Buruo Co, which included an echo-sounder bathymetric survey and collection of sediment cores. A 435 cm-long sediment core (BRLC13-1) and a 65-cm-long core (BRGC13-5) were retrieved from the same site at a water depth of 83.5 m using a piston corer and modified gravity corer, respectively (Fig. 1C). In the laboratory, the upper 20 cm of the gravity core was sliced into 0.5-cm interval, and the remainder of the gravity core and the entire piston core were sliced into 1-cm interval.

3.2. Dating

Gravity core BRGC13-5 was performed on the excessive ^{210}Pb radionuclide activities analyses and ^{137}Cs activities. The measurements were made using high purity germanium gamma spectrometry (ORTEC-GWL-120-15) in the Institute of Tibetan Plateau Research (ITP), Chinese Academy of Sciences. The measurement time for each sample was 8×10^4 s. In addition, 15 samples from different depths of BRLC13-1 core were selected for radiocarbon dating, which was conducted using accelerator mass spectrometry (AMS) by Beta Analytic Inc., U.S.A. The dated material for all samples was bulk organic matter. The radiocarbon ages were converted to calendar ages using the IntCal 13 calibration data (Reimer et al., 2013). An age model for core BRLC13-1 was established using the ^{210}Pb and ^{137}Cs ages for core BRGC13-5 and the 15 ^{14}C ages for core BRLC13-1, using a Bayesian age-depth model (Blaauw and Christen, 2011) implemented with Bacon software.

3.3. Analytical methods of proxies

The total inorganic carbon (TIC) and total carbon (TC) content of samples at a 1-cm interval were measured with a Shimadzu TOC-V_{CPH} carbon analyzer. Total organic carbon (TOC) was calculated as TC-TIC. Total nitrogen (TN) was measured at 1-cm resolution with an Elementar vario MAX cube elemental analyzer.

Grain size analyses were conducted at a 1-cm resolution using a Malvern Mastersizer 3000 laser particle sizer. Samples were pretreated with H_2O_2 and HCl to remove organic matter and carbonate, respectively, before adding Na-hexametaphosphate to disperse aggregates. The mean grain-size was calculated and in addition the proportions of particles within the following size fractions were calculated using GRADISTAT 8.0 software (Blott and Pye, 2001): clay (< 2 μm), very fine silt (2–4 μm), fine silt (4–8 μm), medium silt (8–16 μm), coarse silt (16–32 μm), very coarse silt (32–63 μm) and sand (> 63 μm).

Samples for magnetic susceptibility measurements were prepared by vacuum freeze-drying to prevent possible alteration of the magnetic properties of the sediments. They were then packed in non-magnetic plastic boxes of 10 cm^3 volume and the magnetic susceptibility measured at 1-cm resolution with a Bartington MS2 susceptibility meter and

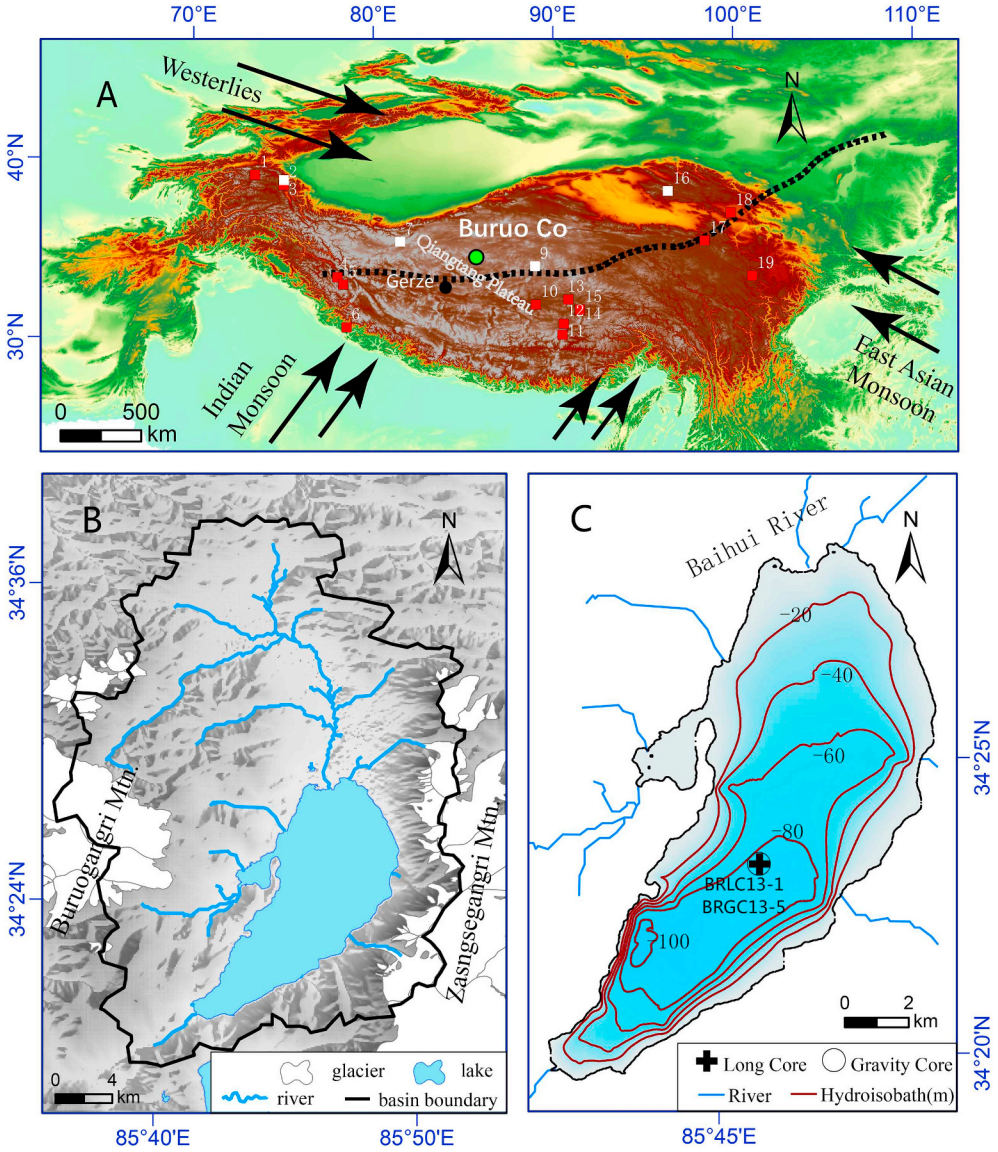

Fig. 1. (A) Sketch maps of the study area of Buruo Co (green dot) and the dotted line indicates the boundary of the westerlies and the Monsoon. Sites of paleoclimate records from glacier and lakes or peats mentioned in this study are marked separately by white and red squares. (B) Hydrographic net of Buruo Co. (C) Bathymetric map of Buruo Co and the core site. (For interpretation of the references to colour in this figure legend, the reader is referred to the web version of this article.)

MS2B sensor. The measurements were repeated at least 3 times to assess their reproducibility.

Element analyses were performed using thermal inductively coupled plasma mass spectrometry (ICP-MS) and inductively coupled plasma optical emission spectrometry (ICP-OES). Samples at 3–5 cm interval were pretreated using pressurized acid digestion with a mixture of HNO_3/HF and measured with ICP-MS (X-7, Thermo-elemental, U.S.A.) and ICP-OES (Prodigy-H, Teledyne Leeman Labs., U.S.A.). All the measurements were conducted at the ITP, Chinese Academy of Sciences.

Forty samples from core BRLC13-1 were selected for pollen analysis. Pretreatment consisted of the following steps: (1) Addition of 1 tablet of *Lycopodium* spores (18,583 grains per tablet) to 5 g of dried sediment to estimate pollen concentration; (2) sequential treatment with 10% HCl, 10% NaOH, 40% HF and acetolysis; and (3) washing through a 10-μm screen to remove clay-sized particles. At least 300 pollen grains were counted for each sample and the identifications were conducted at Nanjing Institute of Geology and Paleontology, Chinese Academy of Sciences.

4. Results

4.1. Chronology

The 15 ^{14}C-derived calendar ages of core BRLC13-1 are listed in Table 1 and the resulting age-depth relationship is shown in Fig. 2A (black dots). Notably, the age for the depth of 1 cm is 3800 yr BP, which indicates a substantial carbon reservoir effect. To investigate the carbon reservoir effect, we compared the difference between the calendar age and the age inferred from the sedimentation rate in the uppermost part of core BRGC13-5. The sedimentation rate for core BRGC13-5, which was retrieved from the same site and at the same time as core BRLC13-1, was determined using the ^{210}Pb Constant Rate of Supply (CRS) model, validated by ^{137}Cs time markers. Based on the CRS model, the age at 1-cm depth was −56 yr BP (Fig. 3) while at the same depth the conventional age converted from the radiocarbon age is 3800 yr BP, indicating a carbon reservoir age of 3856 years in the upper section of core BRLC13-1. We assumed that the carbon reservoir effect was constant throughout the entire sequence, and thus carbon reservoir-

Table 1
AMS ^{14}C Ages and Reservoir-corrected ^{14}C Age by 3856 years for BRLC13-1 core of Buruo Co.

Lab no. (BETA)	Depth (cm)	Materials	$^{13}C/^{12}C$ (‰)	Measured Age (yr BP)	Conventional Age (yr BP)	Reservoir-corrected ^{14}C Age by 3856 years (yr BP)
381697	1	Organic sediment	−26.0	3820 ± 30	3800 ± 30	−56 ± 30
444620	26	Organic sediment	−23.9	5750 ± 30	5770 ± 30	1914 ± 30
435797	50	Organic sediment	−23.4	5310 ± 30	5340 ± 30	1484 ± 30
444621	71	Organic sediment	−22.2	5410 ± 30	5460 ± 30	1604 ± 30
393624	100	Organic sediment	−22.7	5110 ± 30	5150 ± 30	1294 ± 30
435798	150	Organic sediment	−23.5	6110 ± 30	6130 ± 30	2274 ± 30
444622	155	Organic sediment	−22.6	6370 ± 30	6410 ± 30	2554 ± 30
393626	200	Organic sediment	−22.4	5990 ± 30	6030 ± 30	2174 ± 30
444623	234	Organic sediment	−22.5	6580 ± 30	6620 ± 30	2764 ± 30
435799	250	Organic sediment	−23.1	6990 ± 30	7020 ± 30	3164 ± 30
444624	264	Organic sediment	−22.8	6170 ± 30	6210 ± 30	2354 ± 30
393628	299	Organic sediment	−23.0	6910 ± 30	6940 ± 30	3084 ± 30
444625	361	Organic sediment	−22.4	7870 ± 30	7910 ± 30	4054 ± 30
435800	375	Organic sediment	−23.2	7980 ± 30	8010 ± 30	4154 ± 30
381699	436	Organic sediment	−23.9	7120 ± 30	7140 ± 30	3284 ± 30

The basal sample (436 cm) was obtained from the drill bit.

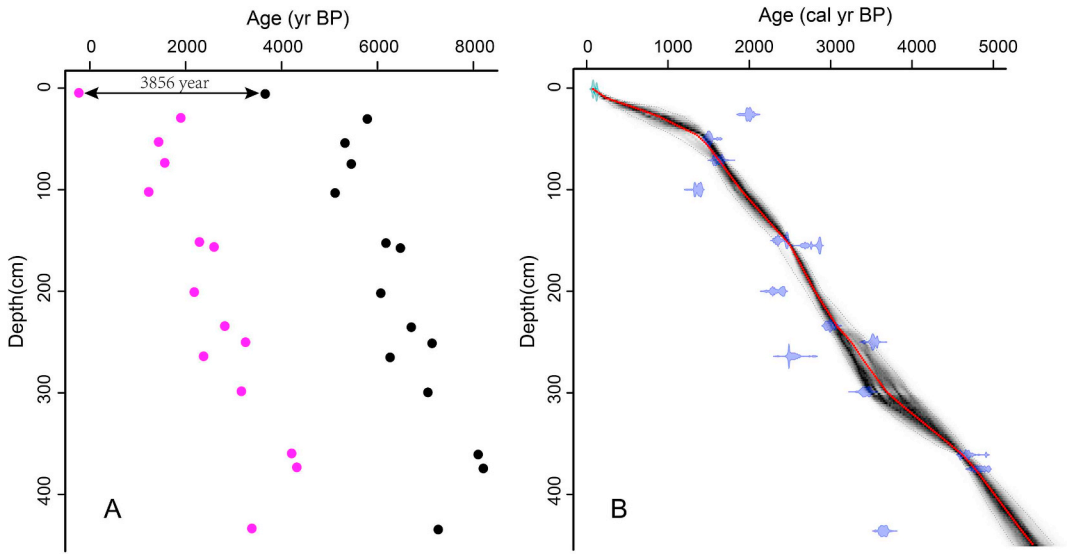

Fig. 2. (A) Age-depth relationship for the sediments of Buruo Co. The black dots are ^{14}C conventional ages and the pink dots are carbon reservoir-corrected obtained by subtracting 3856 years from the ^{14}C conventional ages. (B) Age-depth model for BRLC13-1 of Buruo Co using the Bacon model (Blaauw and Christen, 2011). The probability density of the calibrated result for each conventional radiocarbon date is shown in blue. (For interpretation of the references to colour in this figure legend, the reader is referred to the web version of this article.)

corrected ages were obtained by subtracting 3856 years from the conventional ages (Fig. 2A, pink dots). Finally, a Bayesian age-depth model based on the carbon reservoir-corrected age was produced using Bacon software (Fig. 2B). The resulting basal age of the core is estimated to be 5216 cal yr BP.

4.2. TOC, TN, TOC/TN and TIC

During 5.2–4.0 cal kyr BP the TOC was relatively uniform with minor fluctuations. From 4.0 to 3.3 cal kyr BP, the values fluctuate substantially and reach a maximum at the end of the interval. Subsequently, during 3.3–2.9 cal kyr BP, they decrease rapidly. TN fluctuates slightly during 5.2–3.3 cal kyr BP and then decreases abruptly from ~3.2 cal kyr BP. After reaching relatively low values at 2.9 cal kyr BP, both TOC and TN remain stable with minor fluctuations until 1.7 cal kyr BP. Subsequently, there is a peak in TOC at ~1.4 cal kyr BP. During 5.2–3.2 cal kyr BP the TOC/TN ratio fluctuates from 5.9–9.4 with an average of 7.7. Following a rapid decrease at 3.2 cal kyr BP, the TOC/TN ratio increases slowly, with frequent fluctuations, reaching a peak of 13.3 at 1.5–1.4 cal kyr BP; thereafter, it gradually decreases to 4.9. From 5.2–4.0 cal kyr BP, the TIC is low and fluctuates within a narrow range. Subsequently, it increases with distinct oscillations and reaches a maximum at 1.7 cal kyr BP; finally, from 1.7–1.2 cal kyr BP, it decreases rapidly and then more slowly, with low-amplitude oscillations.

4.3. Grain size

The mean grain size of core BRLC13-1 ranges from 11.6–28.4 μm with an average of 17.9 μm. Analysis with GRADISTAT indicates that all the samples are poorly sorted. The sediments are mainly composed of silt (2–63 μm) with the proportion ranging from 89 to 94%; the average contents of clay (< 2 μm) and sand (> 63 μm) are only 4.5% and 3%, respectively. We divided the silt fraction into three parts: finer silt (2–8 μm), medium silt (8–16 μm) and coarser silt (16–63 μm). The finer silt fraction includes very fine silt (2–4 μm) and fine silt (4–8 μm), and the coarser silt fraction includes coarse silt (16–31 μm) and very coarse silt (31–63 μm).

High-amplitude changes in sand, very coarse silt and medium silt occur during 5.2–3.2 cal kyr BP, while the coarse and finer silt and clay

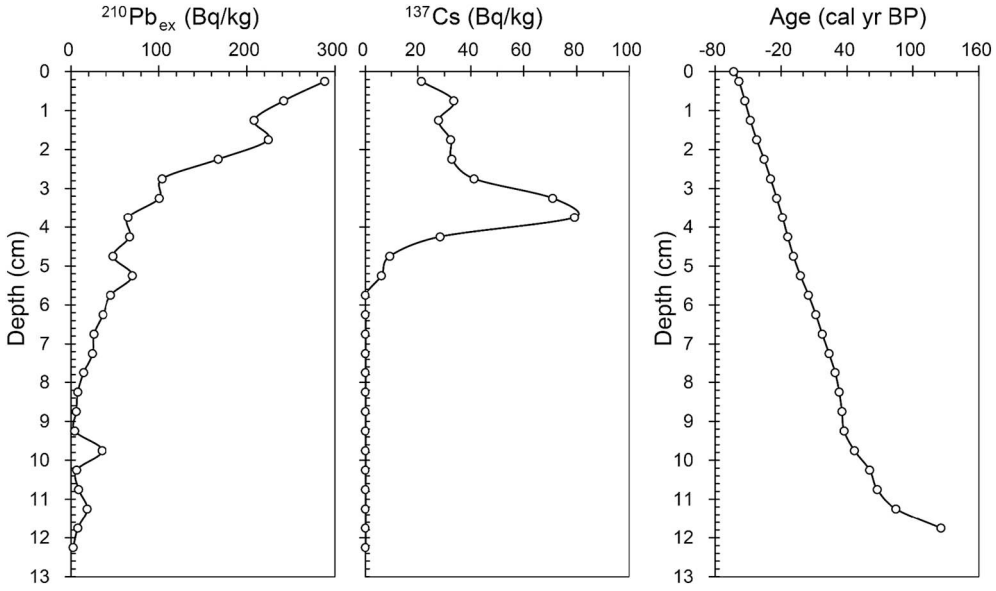

Fig. 3. ^{210}Pb and ^{137}Cs measurements of the upper 13 cm section of BRGC13-5 core and the chronology in this section based on the CRS model.

fluctuate only slightly. Interestingly, while the peaks in mean grain size at 4.9, 4.0, 3.8 and 3.2 cal kyr BP correspond to increases in the content of sand and very coarse silt, the content of medium silt is lower. From 3.2–2.9 cal kyr BP, the mean grain-size decreases, together with an increase in the proportion of finer material and a decrease in the proportion of coarser material. After 2.9 cal kyr BP, the mean grain size decreases slightly, together with a decrease in the proportion of coarse silt. However, the proportions of the other components are relatively stable with very minor fluctuations.

4.4. Magnetic susceptibility

The magnetic susceptibility values of core BRLC13-1 range from 12.1–33.1 $\times 10^{-8}$ $m^3 \cdot kg^{-1}$ (Fig. 4B). From 5.2–2.3 cal kyr BP, the values are generally stable except for two intervals of higher values at 4.8 and 4.0 cal kyr BP. Thereafter, the values increasing substantially and reach a maximum at 2.2 cal kyr BP, before decreasing after 2.1 cal kyr BP, during this latter interval, the average values are relatively low with the lowest value at ~1.3 cal kyr BP.

4.5. Artemisia to Chenopodiaceae (A/C) ratio

The pollen assemblages of core BRLC13-1 are dominated by *Artemisia* (41.2–71.4%) and Chenopodiaceae (10.7–36.9%). During 5.2–3.8 cal kyr BP, high frequencies (61.8–71.4%) of *Artemisia* occur while those of Chenopodiaceae decrease from 19.9–11.2%. Thus, the A/C ratio increases rapidly and reaches a maximum of 6.3 at ~3.8 cal kyr BP. Thereafter, the frequencies of *Artemisia* decrease rapidly to ~42.8% at 2.9 cal kyr BP, while those of Chenopodiaceae increase to 20.1%. During this interval, the A/C ratio decreases substantially from 6.3–2.1. From 2.9–1.8 cal kyr BP, *Artemisia* decreases gradually, whereas Chenopodiaceae increases incrementally; both taxa exhibit high amplitude fluctuations, and in addition the A/C ratio fluctuates substantially and decreases to 1.4. After 1.8 cal kyr BP, *Artemisia* and Chenopodiaceae remain stable, while the A/C ratio fluctuates slightly and reaches a minimum of 1.2 at ~0.2 cal kyr BP.

4.6. Major elements

Based on their stratigraphic variations, the major elements in core BRLC13-1 can be divided into three groups. The first group consists of Ca and Sr which exhibit similar trends. Their values fluctuate frequently but after an interval of stable and low values during 5.2–4.0 cal kyr BP, they gradually increase. From 4.0–1.3 cal kyr BP, they continue to increase with large amplitude fluctuations. Subsequently, they decrease rapidly to minimum values during 1.3–1.2 cal kyr BP, and then fluctuate slightly within a relatively narrow range.

The second group consists of Ti, K, Al, Fe and Rb. The content of these elements increases rapidly during 5.2–4.9 cal kyr BP and maintains a high level during 4.9–4.0 cal kyr BP. During 4.0–1.3 cal kyr BP, they decline substantially with frequent fluctuations, in distinct contrast to the variations of Sr and Ca. Nevertheless, during this overall decreasing trend, all the elements of this second group exhibit peak values at 3.5 cal kyr BP. During 1.3–1.0 cal kyr BP, they increase rapidly and then maintain stable values from 1.0–0.4 cal kyr BP. Subsequently, they all exhibit peak values at 0.2 cal kyr BP but then decrease to minimum values at ~0 cal kyr BP.

The third group consists of Zr and Ba. Both Ba and Zr increase before 4.6 cal kyr BP and then remain stable from 4.6–4.0 cal kyr BP; however, the Zr content is lower on average than before. From 4.0–2.9 cal kyr BP, both Ba and Zr decrease slightly and attain lower values at 3.4 cal kyr BP, before increasing again. From 2.9–1.4 cal kyr BP, they decrease gradually, but with a peak in Zr at 2.2 cal kyr BP. Thereafter, Zr remains stable while Ba exhibits large fluctuations with peaks at 1.2 and 0.2 cal kyr BP, and a minimum at 0 cal kyr BP.

5. Discussion

5.1. Interpretation of the proxies

The variations of the grain size of lake sediments reflect hydrodynamic changes in the catchment (Bird et al., 2014; Stansell et al., 2013). Under a high lake level, the sediment/water interface is generally less disturbed by turbulence induced by fluvial inflows and wave action, and fine grains are deposited in the depocenter (Bird et al., 2014; Zhu et al., 2009). However, given a sufficiently large volume of runoff to the lake, the depocenter may receive an increased quantity of coarse-grained sediments due to the increased transport capacity of the inflowing rivers. Both increased precipitation and/or meltwater influx are the main factors driving the input of coarse-grained sediments to lakes (Mügler et al., 2010). The effect of glacial abrasion of bedrock produces large quantities of silt fraction (Boulton, 1978), which can be transported to proglacial lakes by meltwater runoff. Thus, the variation of the silt fraction of proglacial lake sediments is an effective proxy for

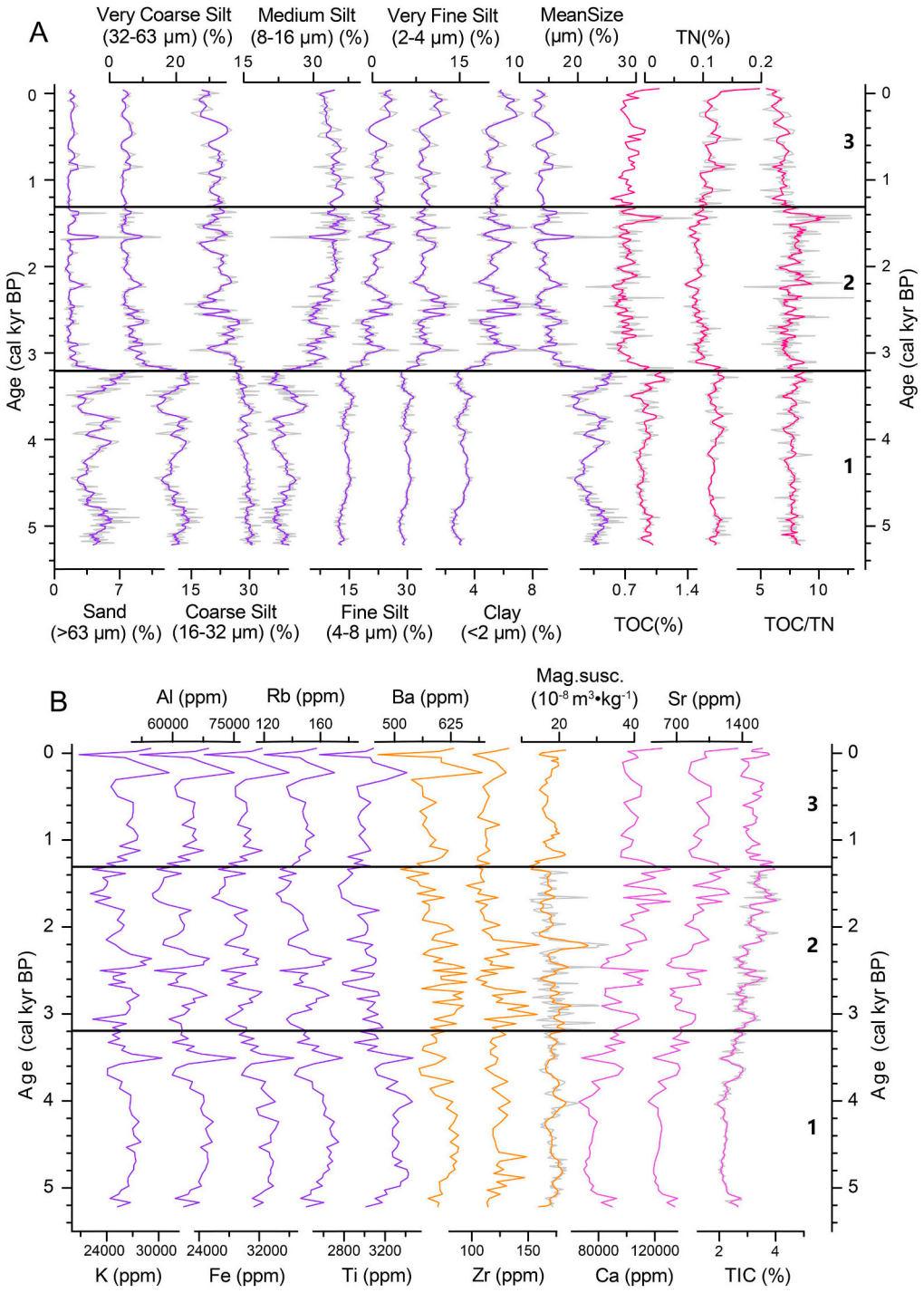

Fig. 4. Proxies derived from the core BRLC13-1 of Buruo Co. The data are smoothed with an eleven-point moving average method. (A) Grain size fraction, TOC, TN and ratio of TOC/TN. (B) Geochemistry elements measured by ICP-MS and ICP-OES, magnetic susceptibility and TIC.

reconstructing the history of glacier activity (Matthews et al., 2000; Nesje et al., 2001). Several researchers have observed that an abundant silt fraction in proglacial lake sediments coincided with strong abrasion beneath wet-based glaciers caused by a glacier advance (Liu et al., 2014; Zhang and Mischke, 2009). Notably, the silt content of the sediments of Buruo Co exceeds 90% and thus we divided it into three fractions: finer silt, medium silt and coarser silt. During periods of glacier retreat, the increased meltwater discharge resulted in increased erosion and transport of surface debris (Ju et al., 2012); on the other hand, however, more surface debris is exposed during a phase of glacier retreat and therefore abundant coarser silt can be transported to the coring site. Conversely, meltwater from the glacier terminus is reduced during a period of glacier advance, and the reduced transport capacity of the meltwater runoff results in an increased proportion of the finer silt fraction (Bianchi and McCave, 1999). Even though glacial erosion may generate a large volume of coarser silt fraction during a period of glacier advance, the weaker transport capacity of the runoff means that much of the coarser silt fraction remains close to the glacier terminus or is confined to the littoral zone of the lake basin. Precipitation also influences the transport of surface debris (Stansell et al., 2014). Notably, the annual precipitation of the Buruo Co catchment is < 200 mm and is concentrated in the meltwater season; thus, the influence of

precipitation is limited to the depocenter of the site, in contrast with that of glacial meltwater. In summary, we infer that increases in the finer silt content of the Buruo Co sediments reflect active erosion associated with a glacier advance, whereas a decrease reflects the retreat of the ice margin.

TOC and TN reflect the accumulation of organic matter, which is contributed by terrestrial and aquatic plants (DoberschŘtz et al., 2014; Meyers, 2003); thus, both are linked to environmental conditions in the catchment and lake environment, with TOC reflecting the air and water temperature and TN reflecting trophic conditions (Zhu et al., 2008). In addition, the TOC/TN ratio can be used to differentiate between various sources of organic matter (Meyers, 2003).

Shifts in the A/C pollen ratio usually reflect changes in moisture availability (El-Moslimany, 1990). In cold alpine areas, *Artemisia* is common and requires high effective moisture, whereas the Chenopodiaceae are adapted to a desert environment (Ma et al., 2017). Both *Artemisia* and Chenopodiaceae are well represented in the pollen spectra of Buruo Co, with their sum exceeding 50%, and therefore the A/C ratio can reliably be used to reconstruct moisture availability (Zhao et al., 2012). Plant growth is closely related to moisture conditions in the catchment; grasses on the Tibetan Plateau rely mainly on rainwater and snowmelt accumulated in the topsoil during the growing season (Hu et al., 2013; Wang et al., 2016), whereas glacier meltwater supplies a relatively narrow zone adjacent to the river. Thus, we infer that the A/C ratio at Buruo Co mainly indicates moisture availability caused by summer precipitation in the catchment.

Ti is a typical in situ residual element concentrated by chemical weathering of bedrock. Changes in the Ti content of sediments reflect changes in the degree of chemical weathering and the sediment transport capacity, hence indirectly they reflect variations in catchment humidity as a function of rainfall (Haug et al., 2001). In the sediments of Buruo Co, the Ti content is significantly correlated with the A/C ratio ($r = 0.775$, $p < 0.01$), indicating that may reflect terrestrial sediment inputs caused by changes in moisture availability linked to precipitation. Since enhanced meltwater influx also occurs in relatively warm periods, which may promote both chemical weathering and materials transport, glacial processes need to be considered when interpreting changes in sedimentary Ti content.

Strong correlations among TIC, Ca and Sr are used to estimate the accumulation of carbonates (DoberschŘtz et al., 2014). In the sediments of Buruo Co, there is strong inverse correlation between Ca and Ti ($r = -0.694$, $p < 0.01$) over the whole sequence which indicates that the carbonates are probably mainly of authigenic origin. At Pumoyum Co, comparison of the Ca content of the water at the lake center with that of the estuary revealed that the Ca content of the lake was substantially influenced by evaporation (Zhu et al., 2010). Therefore, high concentrations of Ca, Sr and TIC can be used to reflect the enrichment of carbonates produced by biological and chemical processes (Daut et al., 2010).

Increases in magnetic susceptibility often reflect the increased input of ferromagnetic minerals resulting from erosion within the catchment (Nesje et al., 2001). In lake catchments containing glaciers, glacial abrasion is the dominant mechanism producing clastic materials in a cold environment (Matthews et al., 2000). If a glacier is near to or adjacent to a lake, the eroded particles may be supplied directly to the lake basin during a glacier advance; however, if the glacier is distant from the lake, clastic materials are generally transported to the lake basin via enhanced meltwater or precipitation. In proglacial lakes on the Tibetan Plateau, positive correlations between glacier advances and high sedimentary magnetic susceptibility are frequently observed (Huang et al., 2016; Liu et al., 2014). In the case of the Buruo Co, glaciers on the east side are close to the lake, but those on the west side are more distant and their influence on the lake sediments would be mediated by meltwater supply to the rivers. Therefore, the fluctuations in the magnetic susceptibility of the sediments of Buruo Co potentially reflect glacier activity, but with a hysteretic effect reflecting the complexity of the processes involved.

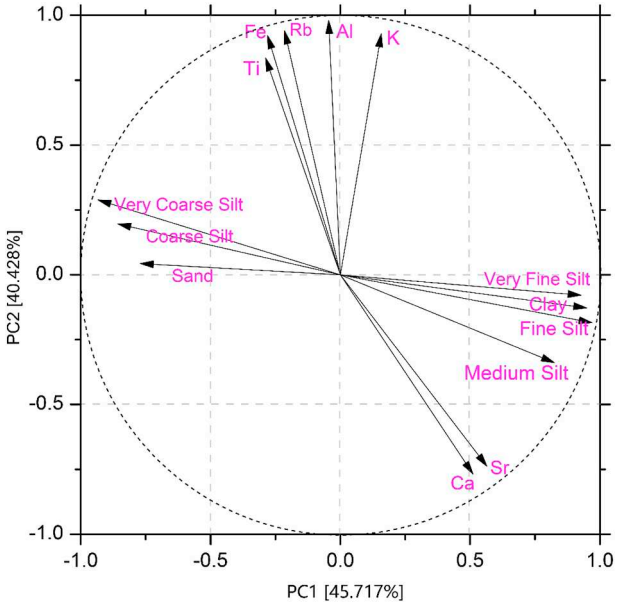

Fig. 5. Principle Component Analysis of the grain size and major elements.

Principal component analysis (PCA) was used to summarize the major trends in the major element and grain-size data. The first two principal components (PC1 and PC2) account for 86.145% of the total variance, with PC1 accounting for 45.717%. A plot of the correlations between the variables and principal components loading diagram (Fig. 5) reveals high positive loadings for Sr, Ca and the finer particles (clay, very fine silt, fine silt and medium silt) on PC1; while the coarser fraction (coarse silt, very coarse silt and sand) has high negative loadings on PC1. We infer that the increasing content of finer particles was mainly influenced by a relatively weak meltwater supply with reduced transport capacity and depositional energy during phases of glacier advance; whereas the content of coarser particles reflects enhanced meltwater transport during phases of glacier retreat. Therefore, PC1 is interpreted as reflecting glacier activity in the Buruo Co catchment, with increases in sample scores on PC1 indicating a glacier advance. PC2 accounts for 40.428% of the total variance and is characterized by high positive correlations with Ti, K, Al, Fe and Rb and negative correlations with Sr and Ca. In general, Ti, Rb, Fe and Al are released by chemical weathering of the substrate and remain as in situ residual materials; thus, they represent allochthonous inputs to the lake basin. In contrast, Sr and Ca are autochthonous components due to their stronger capacity for combining with anions (Kasper et al., 2013). The increase in the allochthonous component reflects stronger surface runoff derived from rainfall or meltwater, which also decreases the ion concentration of the lake water and thus inhibits the precipitation of autochthonous carbonate (Kasper et al., 2012). In addition, the deposition of carbonate reflected by TIC, Sr and Ca is also linked to evaporation and temperature. Therefore, PC2 is interpreted as an index of the interaction of inflowing water and evaporation (I/E).

5.2. Environmental changes during the mid-late Holocene at Buruo Co

The temporal variations in the environmental proxies at Buruo Co enable us to define three stages of environmental evolution since the mid Holocene, which are described below.

During Stage 1 (5.2–3.2 cal kyr BP), the high proportion of coarser silt and relatively small and stable proportion of finer silt indicate a high sediment transport capacity resulting from increasing meltwater supply, which implies glacier retreat under warming conditions. This inference is supported by the high and stable values of TOC and TN,

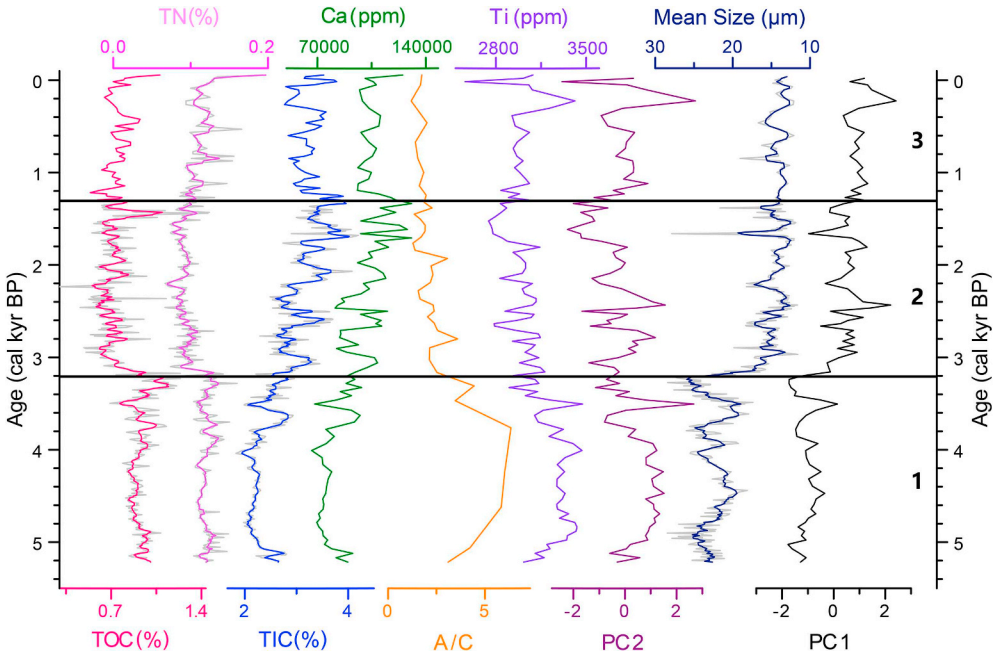

Fig. 6. Plot of the comparison between the A/C ratio, the scores of PC1 and PC2, TOC, TN, TIC, content of Ca and Ti, and mean grain size. The data are smoothed with an 11-point moving average.

which indicate increased biological productivity within the catchment and lake basin. In addition, the increased A/C ratios indicate relatively high precipitation (Fig. 6). An abrupt decrease and lower values of Sr, Ca and TIC at 5.1 cal kyr BP indicate less carbonate deposition because of the enhanced freshwater input from glacial meltwater and rainfall, which may also have resulted in a rising lake level.

However, from 4.0 cal kyr BP, there is a gradual increase in Sr, Ca and TIC which indicates the increased deposition of sedimentary carbonate and that the lake had begun to shrink. This was likely caused by the decreased influx of both glacial meltwater and precipitation which indicates a trend towards cold and dry conditions. The rapid decrease in the A/C ratio also suggests a decrease in moisture availability, and reduced precipitation is also indicated by a decrease in the Ti content and expansion of Chenopodiaceae. In addition, during 4.0–3.2 cal kyr BP there are distinct fluctuations in coarser silt and minor variations in finer silt, indicating unstable climatic conditions.

In summary, during 5.2–4.0 cal kyr BP, the climate was warm and humid, and there was increasing glacial meltwater input. But after 4.0 cal kyr BP, there is a trend towards to dry and cold conditions.

During Stage 2 (3.2–1.3 cal kyr BP), there was a sharp decrease in sand and coarser silt at 3.2 cal kyr BP, and a rapid increase in PC1, medium silt, finer silt and clay during 3.2–2.9 cal kyr BP (Fig. 6). The shift from coarser to finer particles and the steep rise in finer silt indicates that glacial erosion was enhanced but that the transport capacity of the meltwater runoff was limited. This suggests a cold climatic shift at Buruo Co and the rapid expansion of the glaciers in the Zangsegangri and Buruogangri Mountains. The occurrence of colder conditions is also supported by a rapid decrease in TOC from 3.3–2.9 cal kyr BP and a steep fall in TN at 3.2 cal kyr BP, suggesting a rapid decline in biological production within the catchment and a reduction in lake trophic status. Since 2.9 cal kyr BP, the increased scores on PC1, and increased finer silt, medium silt and clay, indicate that glacial abrasion was still strong while the sediment transport capacity was weak due to the reduced meltwater influx and precipitation (Fig. 6). However, the fluctuations in PC1 and PC2 suggest the occurrence of frequent glacial advances and retreats, and they coincide with distinct changes in magnetic susceptibility. The gradual decrease in Ti content and in A/C ratio reflects a decline in moisture availability and low precipitation; similarly, the lower values of TOC and TN indicate a reduced organic matter supply and hence relatively low biological productivity within the lake catchment, probably linked to the deteriorating environment. The steady rise of Sr, Ca and TIC indicate that carbonate accumulation was promoted by a low lake level. Although evaporation was probably limited in the cold conditions, the strong decreases in meltwater and precipitation appear to be the main factor responsible for lake shrinkage.

During this stage, the climate was overall cold and dry and glacier expansion substantially influenced the nature of sedimentation within Buruo Co.

During Stage 3 (1.3–0 cal kyr BP), a rising trend in the proportions of finer silt and clay, and the sample scores on PC1, indicates that glaciers were stable or advancing. Besides, although TN increased substantially from ~1.3 cal kyr BP, the increase in TOC was substantially less, which resulted in a decrease in TOC/TN; hence, there was a decrease in the influx of allochthonous organic carbon. This indicates limited moisture availability at Buruo Co catchment, which is also suggested by the lower A/C ratios (Fig. 6). However, after 1.3 cal kyr BP, the content of Sr, Ca and TIC decreased, while that of Ti, K, Al and Fe increased, suggesting a rise in lake level (Fig. 6). In addition, meltwater influx may have decreased, and the supply of allochthonous elements was influenced mainly by precipitation. Thus, the lake expanded at 1.3 cal kyr BP and the lake level remained stable during 1.2–0 cal kyr BP, which was linked to increased winter precipitation and weak evaporation, implying cold and relatively humid conditions.

5.3. *Glacier variations during the mid-late Holocene on the Tibetan Plateau*

The variations in the fine silt and the scores on PC1, indicate phases of glacier advance and retreat. Four prominent phases of glacial advance are identified in the sedimentary record: during 3.6–3.4 cal kyr BP, 3.2–2.3 cal kyr BP, 1.9–1.7 cal kyr BP and 0.4–0.1 cal kyr BP (Figs. 7, 8E).

5.3.1. *Mid-late Holocene climatic deterioration and Neoglaciation*

After 4.0 cal kyr BP, the variations in Sr, Ca, TIC, A/C ratio and PC2 of Buruo Co sediment suggest a gradual climatic shift to dry conditions,

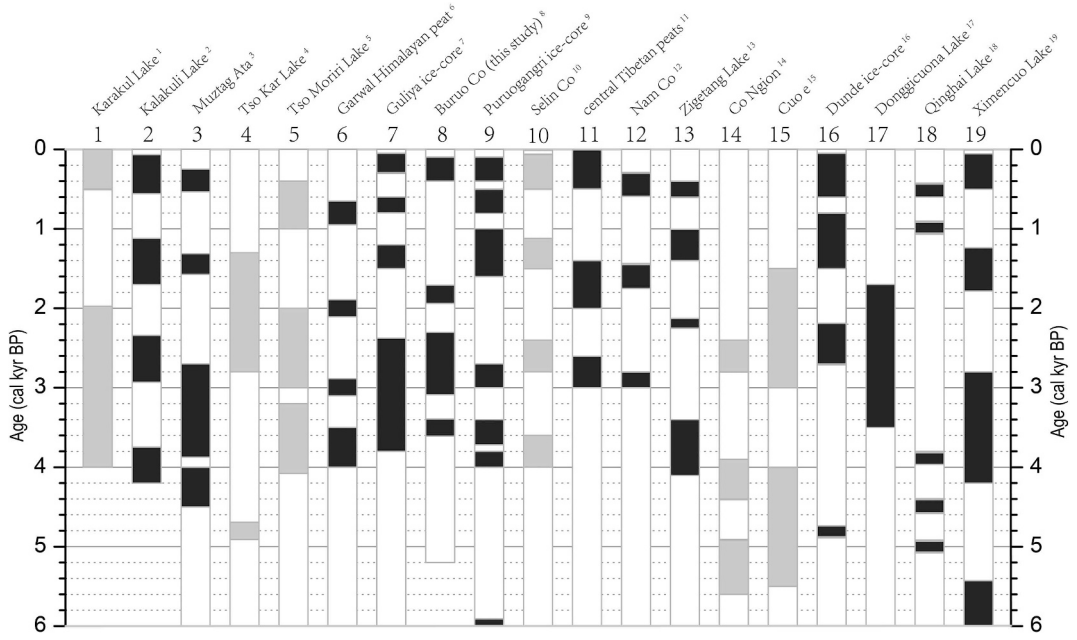

Fig. 7. Timing of the cold (black bars) and dry (gray bars) events recorded in the paleo-environmental archives on Tibetan Plateau and adjacent areas. Reference: 1. Karakul Lake (Taft et al., 2014); 2. Kalakuli Lake (Liu et al., 2014); 3. Glacier record of Muztag Ata and Kongur Shan (Seong et al., 2009); 4. Tso Kar Lake (Demske et al., 2009); 5. Tso Moriri Lake (Leipe et al., 2014); 6. Garwal Himalayan peat (Phadtare, 2000); 7. Guliya ice-core (Thompson et al., 1997); 8. this study; 9. Puruogangri ice-core (Thompson et al., 2006); 10. Selin Co (Shi et al., 2017); 11. Central Tibetan peats (Wang and Fan, 1987); 12. Nam Co (Zhu et al., 2008); 13. Lake Zigetang (Herzschuh et al., 2006); 14. Co Ngion (Leipe et al., 2014); 15. Cuo e (Wu et al., 2006); 16. Dunde ice-core (Liu et al., 1998); 17. Donggicuona Lake (Aichner et al., 2012); 18. Qinghai Lake (Shen et al., 2005); 19. Ximencuo Lake (Mischke and Zhang, 2010). Sites are shown in Fig. 1A as numbered in the description.

accompanied by shrinkage of the lake. Following the onset of a minor glacial advance during 3.6–3.4 cal kyr BP, significant glacier advances occurred during 3.2–2.3 cal kyr BP. Thus, the environmental proxies at Buruo Co suggest a significant climatic deterioration (colder and drier conditions), with the onset of Neoglaciation, characterized by low temperatures and glacier advances.

These cold events are also reflected in several ice-core records. A cold stage during 4.5–2.7 cal kyr BP is evident in glacial records from Muztag Ata and Kongur Shan in the Pamir area (Seong et al., 2009). In addition, lower $\delta^{18}O$ values during 3.8–2.4 cal kyr BP in the Guliya ice core from the northwestern Tibetan Plateau (Thompson et al., 1997) are in accord with the climatic deterioration at Buruo Co, as is the occurrence of cold conditions from 4.0–2.7 cal kyr BP indicated by low $\delta^{18}O$ values in the Puruogangri ice-core from the central Tibetan Plateau (Thompson et al., 2006). Similarly, the pollen record from the Dunde ice-core from the northern Tibetan Plateau indicates a relatively short cold stage from 2.7–2.2 cal kyr BP (Liu et al., 1998).

In addition to the evidence from ice cores from the northern and northwestern Tibetan Plateau, there are numerous records of a cold climatic shift from 4.0–2.9 cal kyr BP from lake sediments (Herzschuh et al., 2006; Zhang and Mischke, 2009) and peat deposits (Phadtare, 2000; Wang and Fan, 1987) (Fig. 7). The sedimentary record of Kalakuli Lake, on the northwestern Tibetan Plateau, indicates glacial advances during 4.2–3.7 cal kyr BP and 2.9–2.4 cal kyr BP (Liu et al., 2014), which is partly consistent with the record from Buruo Co, and fully consistent with the rapid lake fall of Selin Co (Shi et al., 2017) (Fig. 7). These differences may be the result of contrasts between the influences of major controlling system and local climate. In addition, the near absence of ostracods in a sediment core from Tso Kar lake on the eastern Pamir Plateau suggests a change in the status of the lake towards hyperhaline conditions at 3.2 cal kyr BP (Kramer et al., 2014). On the eastern Tibetan Plateau, Schlütz and Lehmkuhl (2009) estimated the age of onset of a Neoglaciation environment at ~4.2 cal kyr BP at Nianbaoyuze Mountain by peat deposits, while the occurrence of colder conditions from 4.2–2.8 cal kyr BP was suggested by Mischke and Zhang (2010). Similarly, a record from Ngangla Ring Tso indicates a shift to dry conditions at ~3.6 cal kyr BP (Hudson et al., 2015). Therefore, the record from Buruo Co, which suggests the onset of climate deterioration at 4.0 cal kyr BP and the Neoglaciation beginning at ~3.2 cal kyr BP, is consistent with records from elsewhere in the region.

5.3.2. *Glacial activity during the last 2000 years*

The record from Buruo Co indicates a glacial advance at 1.9–1.7 cal kyr BP, which may represent the Dark Age Cold Period (DACP). This event is also evident in many lake sediment records from the transition zone between the ISM and the Westerlies, such as Tso Kar Lake on the western Tibetan Plateau (Demske et al., 2009); Selin Co (Shi et al., 2017) and Nam Co (Zhu et al., 2008) on the central Tibetan Plateau; and Donggicuona Lake on the northeastern Tibetan Plateau (Aichner et al., 2012) (Fig. 7). On the northwestern Tibetan Plateau, and in other areas dominated by the Westerlies, a slightly delayed episode of glacial expansion was recorded at Kalakuli Lake during 1.7–1.1 cal kyr BP (Liu et al., 2014), and at Lake Harnur, a glacial lake in the central part of the southern Tianshan Mountains, during 1.8–1.2 cal kyr BP (Lan et al., 2017). On the eastern Tibetan Plateau, there is a record of cold conditions during 1.8–1.3 cal kyr BP from the sediments of Ximencuo Lake (Mischke and Zhang, 2010) and from peat deposits from Nianbaoyuze Mountain (Schlütz and Lehmkuhl, 2009).

At Buruo Co, a recent glacier advance occurred during 0.4–0.1 cal kyr BP, which is likely correlative with the Little Ice Age (LIA). This cold event was also dated to 0.35–0.05 cal kyr BP in the Guliya ice-core (Thompson et al., 1997) and to 0.4–0.1 cal kyr BP in the Puruogangri ice-core (Thompson et al., 2006).

Therefore, the cold conditions of the DACP and LIA, which are reflected in the record from Buruo Co, are substantiated elsewhere, although there are differences in timing, duration and amplitude between different sites. These results suggest that the climatic conditions on the Tibetan Plateau during the mid-late Holocene were probably controlled by the same mechanism, despite the records being located in areas dominated by different atmospheric circulation systems.

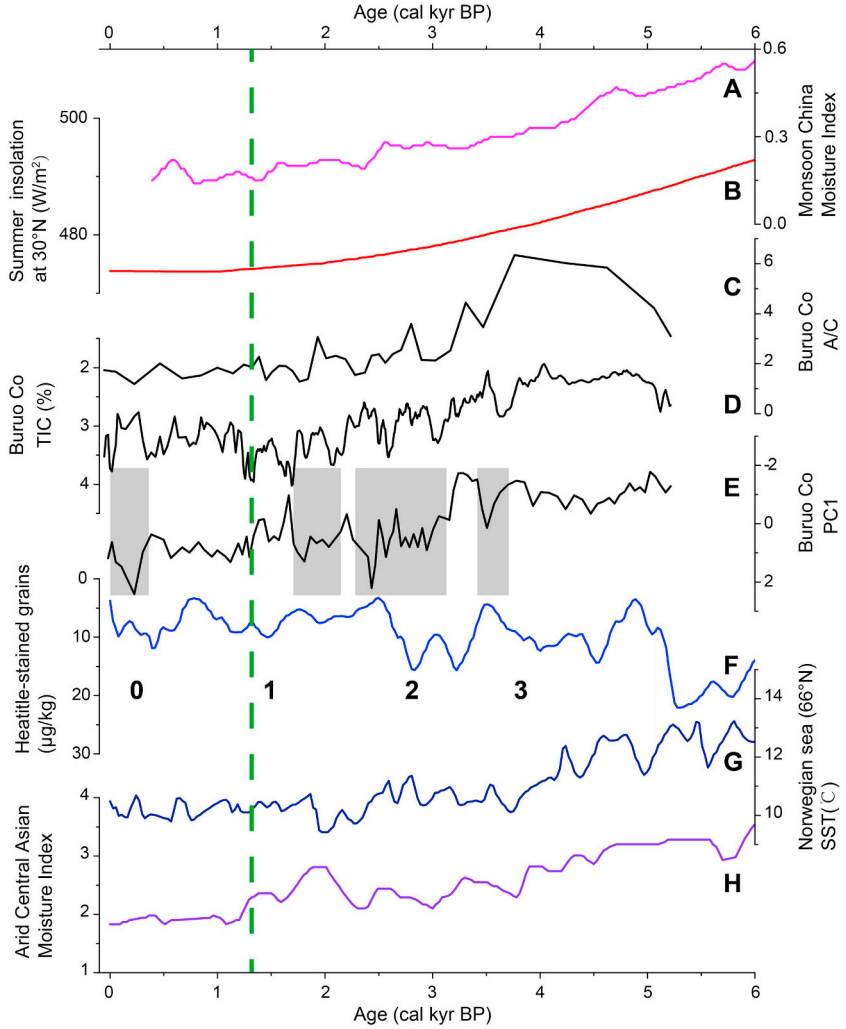

Fig. 8. (A) Monsoon China moisture index (Zhang et al., 2011). (B) the summer (June) insolation at 30°N (Berger and Loutre, 1991). (C) the A/C ratio in Buruo Co. (D) the content of TIC in Buruo Co. (E) the PC1 score in Buruo Co. (F) the hematite-stained grains recorded at the North Atlantic as an indicator of the ice-drift (Bond et al., 2001). (G) the sea surface temperature (SST) at the Norwegian Sea (66°N) (Laskar, 1990). (H) the Arid Central Asian moisture index (Chen et al., 2008).

5.4. *Possible driving mechanisms of climate change and glacial activity*

The overall trend of climate change and glacial activity recorded at Buruo Co is compatible with the secular variation of summer insolation in middle northern latitudes and with the annual temperature of the Northern Hemisphere (Berger and Loutre, 1991; Marcott et al., 2013) (Fig. 8). With the gradual decrease in insolation at 30°N during the mid-Holocene, a significant climatic deterioration occurred from ~4.0 cal kyr BP, which was followed by an extensive and pronounced glacial advance at ~3.2 cal kyr BP. Therefore, we suggest that environmental changes at Buruo Co were mainly driven by variations in summer insolation at ~30°N. Moreover, the climatic deterioration and four glacial advances recoded at Buruo Co correspond well with Bond events 0 to 3, which were cold events in the North Atlantic region (Bond et al., 2001) (Fig. 8F). This suggests a relationship between the climatic conditions at Buruo Co and centennial-scale climatic oscillations in the North Atlantic, mediated by the Westerlies.

The climatic deterioration commenced at 4.0 cal kyr BP at Buruo Co, but there was no significant glacier advance until 3.6 cal kyr BP (Fig. 8). This is different from the record of glacier advance at Muztag Ata which indicates cold conditions around 4.0 cal kyr BP (Fig. 7). However, the enhanced Westerlies could have brought moisture to the northwestern Tibetan Plateau during times when the ISM became weaker. However, the Buruo Co catchment is located in the cold and arid core area of the Tibetan Plateau which would limit the supply of moisture from a weaker ISM and Westerlies, as a result of the topography. The Westerlies is too weak to supply moisture to the Qiangtang Plateau and thus no significant glacier advance occurred in the Buruo Co catchment under the cold and dry conditions around 4.0 cal kyr BP. Therefore, we suggest that, prior to 4.0 cal kyr BP, the environmental conditions at Buruo Co were controlled by the combination of a stronger ISM and weak Westerlies, and that Westerlies influence was only gradually enhanced after 3.2 cal kyr BP.

The moisture index for monsoon China (Zhang et al., 2011) and the summer insolation at middle latitudes exhibit a similar decreasing trend during 4.0–1.3 cal kyr BP, indicating that the weak ISM was linked with the continuously decreasing summer insolation at 30°N. The decreased ISM rainfall, reduced meltwater influx and low temperatures, linked to insolation changes, were likely the main causes of the shrinkage of Buruo Co during 4.0–1.3 cal kyr BP. Thus, we infer that the northern Qiangtang Plateau was mainly controlled by strong Westerlies circulation and a weak ISM during this period.

After 1.3 cal kyr BP, there was a minor increase in the moisture status of Buruo Co (Fig. 8D), which is in accord with many coeval records of the occurrence of cold and humid conditions in the northwestern Tibetan Plateau (Fig. 7). During this stage, increases in sea-surface temperatures in the North Atlantic and in air temperatures at high northern latitudes may have resulted in enhanced evaporation,

resulting in increased moisture transport by the Westerlies to arid central Asia (Chen et al., 2008). The increased precipitation not only caused an increase in water input, but also provided a source for glacier expansion under the conditions of lower insolation. Therefore, the scale of the glaciers may have expanded and the lake level increased from 1.3 cal kyr BP at Buruo Co, under the prevailing Westerlies circulation.

6. Conclusions

We have used records of various environmental proxies (grain size, TOC, TIC, Ti and A/C ratios) from the sediments of proglacial lake Buruo Co on the northern Tibetan Plateau to reconstruct the history of climate change and glacial activity since 5.2 cal kyr BP.

During 5.2–4.0 cal kyr BP, the climate was relatively warm and wet, and retreating glaciers released large amounts of freshwater, which together with the abundant precipitation maintained a high lake level. Environmental conditions at this time were controlled by a relatively strong ISM (which transported moisture to the area) and relatively weak Westerlies. During 4.0–1.3 cal kyr BP, colder and drier conditions developed, glaciers expanded, and the lake level decreased in response to the decreased water input. These conditions reflect the prevailing influence of the gradually enhancing Westerlies. During 1.3–0 cal kyr BP, the enhanced Westerlies transported more moisture to Buruo Co, leading to the development of relatively large glaciers under the prevailing cold conditions. The lake level rose after 1.3 cal kyr BP, probably in response to increased precipitation.

Climatic deterioration occurred at 4.0 cal kyr BP and four glacier advances (3.6–3.4 cal kyr BP, 3.2–2.3 cal kyr BP, 1.9–1.7 cal kyr BP, 0.4–0.1 cal kyr BP) are recorded by the sediments of Buruo Co. These advances are correlative with variations in insolation at 30°N and with Bond events in the North Atlantic, which indicates that climate change and glacial activity at Buruo Co were dominantly influenced by variations in Northern Hemisphere insolation and by climatic oscillations in the North Atlantic region, possibly via the Westerlies circulation.

Acknowledgments

This work was supported by the CAS Strategic Priority Research Program (grant number XDA20020100); NSFC project (grant number 41831177); CAS International Partnership Program (131C11KYSB20160061); the 13th Five-year Informatization Plan of Chinese Academy of Sciences (XXH13505-06). We would like to thank Yong Wang, Xiao Lin, Xing Hu and Ruyi Wei for their assistance in the field. We are grateful to Lingyu Tang for his support and help in sample treatments. The authors thank Editor Paul Hesse, Dr. Xuhua Shi and one anonymous reviewer for providing constructive comments that improved the manuscript.

References

Aichner, B., Herzschuh, U., Wilkes, H., Schulz, H.-M., Wang, Y., Plessen, B., Mischke, S., Diekmann, B., Zhang, C., 2012. Ecological development of Lake Donggi Cona, northeastern Tibetan Plateau, since the late glacial on basis of organic geochemical proxies and non-pollen palynomorphs. Palaeogeogr. Palaeoclimatol. Palaeoecol. 313, 140–149.

An, Z., Kutzbach, J.E., Prell, W.L., Porter, S.C., 2001. Evolution of Asian monsoons and phased uplift of the Himalaya–Tibetan plateau since Late Miocene times. Nature 411, 62–66.

Berger, A., Loutre, M.-F., 1991. Insolation values for the climate of the last 10 million years. Quat. Sci. Rev. 10, 297–317.

Bianchi, G.G., McCave, I.N., 1999. Holocene periodicity in North Atlantic climate and deep-ocean flow south of Iceland. Nature 397, 515.

Bird, B.W., Polisar, P.J., Lei, Y., Thompson, L.G., Yao, T., Finney, B.P., Bain, D.J., Pompeani, D.P., Steinman, B.A., 2014. A Tibetan lake sediment record of Holocene Indian summer monsoon variability. Earth Planet. Sci. Lett. 399, 92–102.

Blaauw, M., Christen, J.A., 2011. Flexible paleoclimate age-depth models using an autoregressive gamma process. Bayesian Anal. 6, 457–474.

Blott, S.J., Pye, K., 2001. GRADISTAT: a grain size distribution and statistics package for the analysis of unconsolidated sediments. Earth Surf. Process. Landf. 26, 1237–1248.

Bond, G., Kromer, B., Beer, J., Muscheler, R., Evans, M.N., Showers, W., Hoffmann, S., Lotti-Bond, R., Hajdas, I., Bonani, G., 2001. Persistent solar influence on North Atlantic climate during the Holocene. Science 294, 2130–2136.

Boulton, G., 1978. Boulder shapes and grain-size distributions of debris as indicators of transport paths through a glacier and till genesis. Sedimentology 25, 773–799.

Chen, F., Yu, Z., Yang, M., Ito, E., Wang, S., Madsen, D.B., Huang, X., Zhao, Y., Sato, T., John, B., Birks, H., Boomer, I., Chen, J., An, C., Wünnemann, B., 2008. Holocene moisture evolution in arid central Asia and its out-of-phase relationship with Asian monsoon history. Quat. Sci. Rev. 27, 351–364.

Daut, G., Mäusbacher, R., Baade, J., Gleixner, G., Kroemer, E., Mügler, I., Wallner, J., Wang, J., Zhu, L., 2010. Late Quaternary hydrological changes inferred from lake level fluctuations of Nam Co (Tibetan Plateau, China). Quat. Int. 218, 86–93.

Demske, D., Tarasov, P.E., Wünnemann, B., Riedel, F., 2009. Late glacial and Holocene vegetation, Indian monsoon and westerly circulation in the Trans-Himalaya recorded in the lacustrine pollen sequence from Tso Kar, Ladakh, NW India. Palaeogeogr. Palaeoclimatol. Palaeoecol. 279, 172–185.

DoberschŘtz, S., Frenzel, P., Haberzettl, T., Kasper, T., Wang, J., Zhu, L., Daut, G., Schwalb, A., Mńusbacher, R., 2014. Monsoonal forcing of Holocene paleoenvironmental change on the central Tibetan Plateau inferred using a sediment record from Lake Nam Co (Xizang, China). J. Paleolimnol. 51, 253–266.

El-Moslimany, A.P., 1990. Ecological significance of common nonarboreal pollen: examples from drylands of the Middle East. Rev. Palaeobot. Palynol. 64, 343–350.

Haug, G.H., Hughen, K.A., Sigman, D.M., Peterson, L.C., Röhl, U., 2001. Southward migration of the intertropical convergence zone through the Holocene. Science 293, 1304–1308.

Herzschuh, U., Winter, K., Wünnemann, B., Li, S., 2006. A general cooling trend on the central Tibetan Plateau throughout the Holocene recorded by the Lake Zigetang pollen spectra. Quat. Int. 154, 113–121.

Holzhauser, H., Magny, M., Zumbuühl, H.J., 2005. Glacier and lake-level variations in west-central Europe over the last 3500 years. The Holocene 15, 789–801.

Hou, J., D'Andrea, W.J., Wang, M., He, Y., Liang, J., 2017. Influence of the Indian monsoon and the subtropical jet on climate change on the Tibetan Plateau since the late Pleistocene. Quat. Sci. Rev. 163, 84–94.

Hu, J., Hopping, K.A., Bump, J.K., Kang, S., Klein, J.A., 2013. Climate change and water use partitioning by different plant functional groups in a grassland on the Tibetan Plateau. PLoS One 8, e75503.

Huang, L., Zhu, L., Wang, J., Ju, J., Wang, Y., Zhang, J., Yang, R., 2016. Glacial activity reflected in a continuous lacustrine record since the early Holocene from the proglacial Laigu Lake on the southeastern Tibetan Plateau. Palaeogeogr. Palaeoclimatol. Palaeoecol. 456, 37–45.

Hudson, A.M., Quade, J., Huth, T.E., Lei, G., Cheng, H., Edwards, L.R., Olsen, J.W., Zhang, H., 2015. Lake level reconstruction for 12.8–2.3 ka of the Ngangla Ring Tso closed-basin lake system, southwest Tibetan Plateau. Quat. Res. 83, 66–79.

Immerzeel, W.W., Van Beek, L.P., Bierkens, M.F., 2010. Climate change will affect the Asian water towers. Science 328, 1382–1385.

Joerin, U.E., Stocker, T.F., Schlüchter, C., 2006. Multicentury glacier fluctuations in the Swiss Alps during the Holocene. The Holocene 16, 697–704.

Ju, J., Zhu, L., Feng, J., Wang, J., Wang, Y., Xie, M., Peng, P., Zhen, X., Lü, X., 2012. Hydrodynamic process of Tibetan Plateau lake revealed by grain size: case study of Pumayum Co. Chin. Sci. Bull. 57, 2433–2441.

Karlén, W., 1976. Lacustrine sediments and tree-limit variations as indicators of Holocene climatic fluctuations in Lappland, northern Sweden. Geogr. Ann. Ser. B 58, 1–34.

Kasper, T., Haberzettl, T., Doberschütz, S., Daut, G., Wang, J., Zhu, L., Nowaczyk, N., Mäusbacher, R., 2012. Indian Ocean Summer Monsoon (IOSM)-dynamics within the past 4 ka recorded in the sediments of Lake Nam Co, central Tibetan Plateau (China). Quat. Sci. Rev. 39, 73–85.

Kasper, T., Frenzel, P., Haberzettl, T., Schwarz, A., Daut, G., Meschner, S., Wang, J., Zhu, L., Mäusbacher, R., 2013. Interplay between redox conditions and hydrological changes in sediments from Lake Nam Co (Tibetan Plateau) during the past 4000cal BP inferred from geochemical and micropaleontological analyses. Palaeogeogr. Palaeoclimatol. Palaeoecol. 392, 261–271.

Kramer, M., Kotlia, B., Wünnemann, B., 2014. A late quaternary ostracod record from the Tso Kar basin (North India) with a note on the distribution of recent species. J. Paleolimnol. 51, 549–565.

Lan, J., Xu, H., Sheng, E., Yu, K., Wu, H., Zhou, K., Yan, D., Ye, Y., Wang, T., 2017. Climate changes reconstructed from a glacial lake in High Central Asia over the past two millennia. Quat. Int. 1–11.

Laskar, J., 1990. The chaotic motion of the solar system: a numerical estimate of the size of the chaotic zones. Icarus 88, 266–291.

Leipe, C., Demske, D., Tarasov, P.E., 2014. A Holocene pollen record from the northwestern Himalayan lake Tso Moriri: implications for palaeoclimatic and archaeological research. Quat. Int. 348, 93–112.

Leonard, E.M., 1986. Varve studies at Hector Lake, Alberta, Canada, and the relationship between glacial activity and sedimentation. Quat. Res. 25, 199–214.

Liu, K.-b., Yao, Z., Thompson, L.G., 1998. A pollen record of Holocene climatic changes from the Dunde ice cap, Qinghai-Tibetan Plateau. Geology 26, 135–138.

Liu, X., Herzschuh, U., Wang, Y., Kuhn, G., Yu, Z., 2014. Glacier fluctuations of Muztagh Ata and temperature changes during the late Holocene in westernmost Tibetan Plateau, based on glaciolacustrine sediment records. Geophys. Res. Lett. 41, 6265–6273.

Liu, J., Yi, C., Li, Y., Bi, W., Zhang, Q., Hu, G., 2017. Glacial fluctuations around the Karola Pass, eastern Lhagoi Kangri Range, since the Last Glacial Maximum. J. Quat. Sci. 32, 516–527.

Loso, M.G., 2009. Summer temperatures during the Medieval Warm Period and Little Ice Age inferred from varved proglacial lake sediments in southern Alaska. J. Paleolimnol. 41, 117.

Loso, M.G., Anderson, R.S., Anderson, S.P., Reimer, P.J., 2006. A 1500-year record of

temperature and glacial response inferred from varved Iceberg Lake, southcentral Alaska. Quat. Res. 66, 12–24.
Ma, Q., Zhu, L., Wang, J., Ju, J., Lu, X., Wang, Y., Guo, Y., Yang, R., Kasper, T., Haberzettl, T., Tang, L., 2017. Artemisia/Chenopodiaceae ratio from surface lake sediments on the central and western Tibetan Plateau and its application. Palaeogeogr. Palaeoclimatol. Palaeoecol. 479, 138–145.
Marcott, S.A., Shakun, J.D., Clark, P.U., Mix, A.C., 2013. A reconstruction of regional and global temperature for the past 11,300 years. Science 339, 1198–1201.
Matthews, J.A., Dahl, S.O., Nesje, A., Berrisford, M.S., Andersson, C., 2000. Holocene glacier variations in central Jotunheimen, southern Norway based on distal glacio-lacustrine sediment cores. Quat. Sci. Rev. 19, 1625–1647.
Meyers, P.A., 2003. Applications of organic geochemistry to paleolimnological reconstructions: a summary of examples from the Laurentian Great Lakes. Org. Geochem. 34, 261–289.
Mischke, S., Zhang, C., 2010. Holocene cold events on the Tibetan Plateau. Glob. Planet. Chang. 72, 155–163.
Mügler, I., Gleixner, G., Günther, F., Mäusbacher, R., Daut, G., Schütt, B., Berking, J., Schwalb, A., Schwark, L., Xu, B., 2010. A multi-proxy approach to reconstruct hydrological changes and Holocene climate development of Nam Co, Central Tibet. J. Paleolimnol. 43, 625–648.
Nesje, A., Matthews, J.A., Dahl, S.O., Berrisford, M.S., Andersson, C., 2001. Holocene glacier fluctuations of Flatebreen and winter-precipitation changes in the Jostedalsbreen region, western Norvay, based on glaciolacustrine sediment records. The Holocene 11, 267–280.
Oerlemans, J., 2005. Extracting a climate signal from 169 glacier records. Science 308, 675–677.
Owen, L.A., 2009. Latest Pleistocene and Holocene glacier fluctuations in the Himalaya and Tibet. Quat. Sci. Rev. 28, 2150–2164.
Phadtare, N.R., 2000. Sharp decrease in summer monsoon strength 4000–3500 cal yr BP in the Central Higher Himalaya of India based on pollen evidence from alpine peat. Quat. Res. 53, 122–129.
Pritchard, H.D., 2017. Addendum: editorial expression of concern: Asia's glaciers are a regionally important buffer against drought. Nature 550, 548.
Qinghai-Tibet Plateau Comprehensive Scientific Expedition Team of the Chinese Academy of Sciences, 1992. Tibet Steppe. Science Press, Beijing, China (in Chinese).
Qiu, J., 2008. China: the third pole. Nat. News 454, 393–396.
Reimer, P.J., Bard, E., Bayliss, A., Beck, J.W., Blackwell, P.G., Ramsey, C.B., Buck, C.E., Cheng, H., Edwards, R.L., Friedrich, M., 2013. IntCal13 and Marine13 radiocarbon age calibration curves 0–50,000 years cal BP. Radiocarbon 55, 1869–1887.
Schlütz, F., Lehmkuhl, F., 2009. Holocene climatic change and the nomadic Anthropocene in Eastern Tibet: palynological and geomorphological results from the Nianbaoyeze Mountains. Quat. Sci. Rev. 28, 1449–1471.
Seong, Y.B., Owen, L.A., Yi, C., Finkel, R.C., 2009. Quaternary glaciation of Muztag Ata and Kongur Shan: evidence for glacier response to rapid climate changes throughout the Late Glacial and Holocene in westernmost Tibet. Geol. Soc. Am. Bull. 121, 348–365.
Shen, J., Liu, X., Wang, S., Matsumoto, R., 2005. Palaeoclimatic changes in the Qinghai Lake area during the last 18,000 years. Quat. Int. 136, 131–140.
Shi, X., Kirby, E., Furlong, K.P., Meng, K., Robinson, R., Lu, H., Wang, E., 2017. Rapid and punctuated Late Holocene recession of Siling Co, central Tibet. Quat. Sci. Rev. 172, 15–31.
Simonneau, A., Chapron, E., Garçon, M., Winiarski, T., Graz, Y., Chauvel, C., Debret, M., Motelica-Heino, M., Desmet, M., Di Giovanni, C., 2014. Tracking Holocene glacial and high-altitude alpine environments fluctuations from minerogenic and organic markers in proglacial lake sediments (Lake Blanc Huez, Western French Alps). Quat. Sci. Rev. 89, 27–43.
Stansell, N.D., Rodbell, D.T., Abbott, M.B., Mark, B.G., 2013. Proglacial lake sediment records of Holocene climate change in the western Cordillera of Peru. Quat. Sci. Rev. 70, 1–14.
Stansell, N.D., Polissar, P.J., Abbott, M.B., Bezada, M., Steinman, B.A., Braun, C., 2014. Proglacial lake sediment records reveal Holocene climate changes in the Venezuelan Andes. Quat. Sci. Rev. 89, 44–55.
Taft, L., Mischke, S., Wiechert, U., Leipe, C., Rajabov, I., Riedel, F., 2014. Sclerochronological oxygen and carbon isotope ratios in Radix (Gastropoda) shells indicate changes of glacial meltwater flux and temperature since 4,200 cal yr BP at Lake Karakul, eastern Pamirs (Tajikistan). J. Paleolimnol. 52, 27–41.
Thompson, L.o., Yao, T., Davis, M., Henderson, K., Mosley-Thompson, E., Lin, P.-N., Beer, J., Synal, H.-A., Cole-Dai, J., Bolzan, J., 1997. Tropical climate instability: the last glacial cycle from a Qinghai-Tibetan ice core. Science 276, 1821–1825.
Thompson, L.G., Yao, T., Mosley-Thompson, E., Davis, M., Henderson, K., Lin, P.-N., 2000. A high-resolution millennial record of the South Asian monsoon from Himalayan ice cores. Science 289, 1916–1919.
Thompson, L.G., Tandong, Y., Davis, M.E., Mosley-Thompson, E., Mashiotta, T.A., Lin, P.-N., Mikhalenko, V.N., Zagorodnov, V.S., 2006. Holocene climate variability archived in the Puruogangri ice cap on the central Tibetan Plateau. Ann. Glaciol. 43, 61–69.
Tian, L., Yao, T., MacClune, K., White, J., Schilla, A., Vaughn, B., Vachon, R., Ichiyanagi, K., 2007. Stable isotopic variations in west China: a consideration of moisture sources. J. Geophys. Res. Atmos. 112, 1–12.
Vincent, C., Le Meur, E., Six, D., Funk, M., 2005. Solving the paradox of the end of the Little Ice Age in the Alps. Geophys. Res. Lett. 32, 1–4.
Wang, S., Dou, H., 1998. China Lake Records. Science Press, Beijing, China (in Chinese).
Wang, F., Fan, C., 1987. Climatic changes in the Qinghai-Xizang (Tibetan) region of China during the Holocene. Quat. Res. 28, 50–60.
Wang, Y., Zhu, L., Wang, J., Ju, J., Peng, P., Lin, X., Hu, J., Nishimura, M., 2016. Paleohydrological processes revealed by n-alkane δD in lacustrine sediments of Lake Pumoyum Co, southern Tibetan Plateau, and their response to climate changes during the past 18.5 cal ka. J. Paleolimnol. 56, 223–238.
Wu, Y., Lücke, A., Jin, Z., Wang, S., Schleser, G.H., Battarbee, R.W., Weilan, X., 2006. Holocene climate development on the central Tibetan Plateau: a sedimentary record from Cuoe Lake. Palaeogeogr. Palaeoclimatol. Palaeoecol. 234, 328–340.
Yao, T., Thompson, L., Yang, W., Yu, W., Gao, Y., Guo, X., Yang, X., Duan, K., Zhao, H., Xu, B., 2012. Different glacier status with atmospheric circulations in Tibetan Plateau and surroundings. Nat. Clim. Chang. 2, 663–667.
Yi, C., Chen, H., Yang, J., Liu, B., Fu, P., Liu, K., Li, S., 2008. Review of Holocene glacial chronologies based on radiocarbon dating in Tibet and its surrounding mountains. J. Quat. Sci. 23, 533–543.
You, C., 2016. Historical Biomass Burning Records in the Zangsegangri Ice Core. University of Chinese Academy of Sciences, Beijing (in Chinese).
Zhang, C., Mischke, S., 2009. A Lateglacial and Holocene lake record from the Nianbaoyeze Mountains and inferences of lake, glacier and climate evolution on the eastern Tibetan Plateau. Quat. Sci. Rev. 28, 1970–1983.
Zhang, J., Chen, F., Holmes, J.A., Li, H., Guo, X., Wang, J., Li, S., Lü, Y., Zhao, Y., Qiang, M., 2011. Holocene monsoon climate documented by oxygen and carbon isotopes from lake sediments and peat bogs in China: a review and synthesis. Quat. Sci. Rev. 30, 1973–1987.
Zhao, Y., Liu, H., Li, F., Huang, X., Sun, J., Zhao, W., Herzschuh, U., Tang, Y., 2012. Application and limitations of the Artemisia/Chenopodiaceae pollen ratio in arid and semi-arid China. The Holocene 22, 1385–1392.
Zheng, D., 1996. The System of Physico-Geographical Regions of the Qinghai-Xizang (Tibet) Plateau. (in Chinese).
Zhu, L., Wu, Y., Wang, J., Lin, X., Ju, J., Xie, M., Li, M., Mäusbacher, R., Schwalb, A., Daut, G., 2008. Environmental changes since 8.4 ka reflected in the lacustrine core sediments from Nam Co, central Tibetan Plateau, China. The Holocene 18, 831–839.
Zhu, L., Zhen, X., Wang, J., Lü, H., Xie, M., Kitagawa, H., Possnert, G., 2009. A~ 30,000-year record of environmental changes inferred from Lake Chen Co, Southern Tibet. J. Paleolimnol. 42, 343–358.
Zhu, L., Ju, J., Wang, Y., Xie, M., Wang, J., Peng, P., Zhen, X., Lin, X., 2010. Composition, spatial distribution, and environmental significance of water ions in Pumayum Co catchment, southern Tibet. J. Geogr. Sci. 20, 109–120.